



Valorization of Wastepaper Through Antimicrobial Functionalization with Biogenic Silver Nanoparticles, a Sustainable Packaging Composite

Ozioma Forstinus Nwabor^{1,2} · Sudarshan Singh² · Julalak Chorachoo Ontong^{2,3} · Kitiya Vongkamjan⁴ · Supayang Piyawan Voravuthikunchai²

Received: 11 April 2020 / Accepted: 7 September 2020 / Published online: 10 September 2020
© Springer Nature B.V. 2020

Abstract

Wood pulping for paper production accounts for bulk of the tree lost, with numerous adverse effects to the environment. In this study, *Eucalyptus camaldulensis* leaf extract was used for silver nanoparticles synthesis. The nanoparticles were used as functional agent for the valorization of wastepaper. The nanocomposite paper was characterized for physicochemical, antibacterial and cytotoxicity. DLS and TEM revealed a spherical nano-sized particle with effective diameters of 138.6 nm and mean size of 13.11 nm, respectively while zeta potential was -35.85 mV. Minimum inhibitory and minimum bactericidal concentrations of silver nanoparticles ranged from 0.99 to 1.99 $\mu\text{g/mL}$ and 3.98–15.91 $\mu\text{g/mL}$ respectively. UV–vis spectra presented a peak at 427 nm, indicating the surface plasmon resonance band of silver in the paper. SEM and EDX showed uniform distribution of silver nanoparticles, whereas EDX and ICP-OES results indicated Ag concentration of 0.1%Wt and 0.0112 $\mu\text{g/cm}^2$, respectively. Antibacterial efficacy of the paper demonstrated a bactericidal effect against *Bacillus cereus* and *Escherichia coli* O157:H7 with >3 log reduction in CFU/mL after 3 h of treatment and bacteriostatic effect against *Listeria monocytogenes* and *Staphylococcus aureus*. In addition, cytotoxicity against HEK293T and Caco-2 cells revealed $>80\%$ cell viability. Results indicate that valorization of wastepaper through functionalization with bioactive silver nanoparticles could serve as a sustainable waste management approach.

Electronic supplementary material The online version of this article (<https://doi.org/10.1007/s12649-020-01237-5>) contains supplementary material, which is available to authorized users.

✉ Supayang Piyawan Voravuthikunchai
supayang.v@psu.ac.th

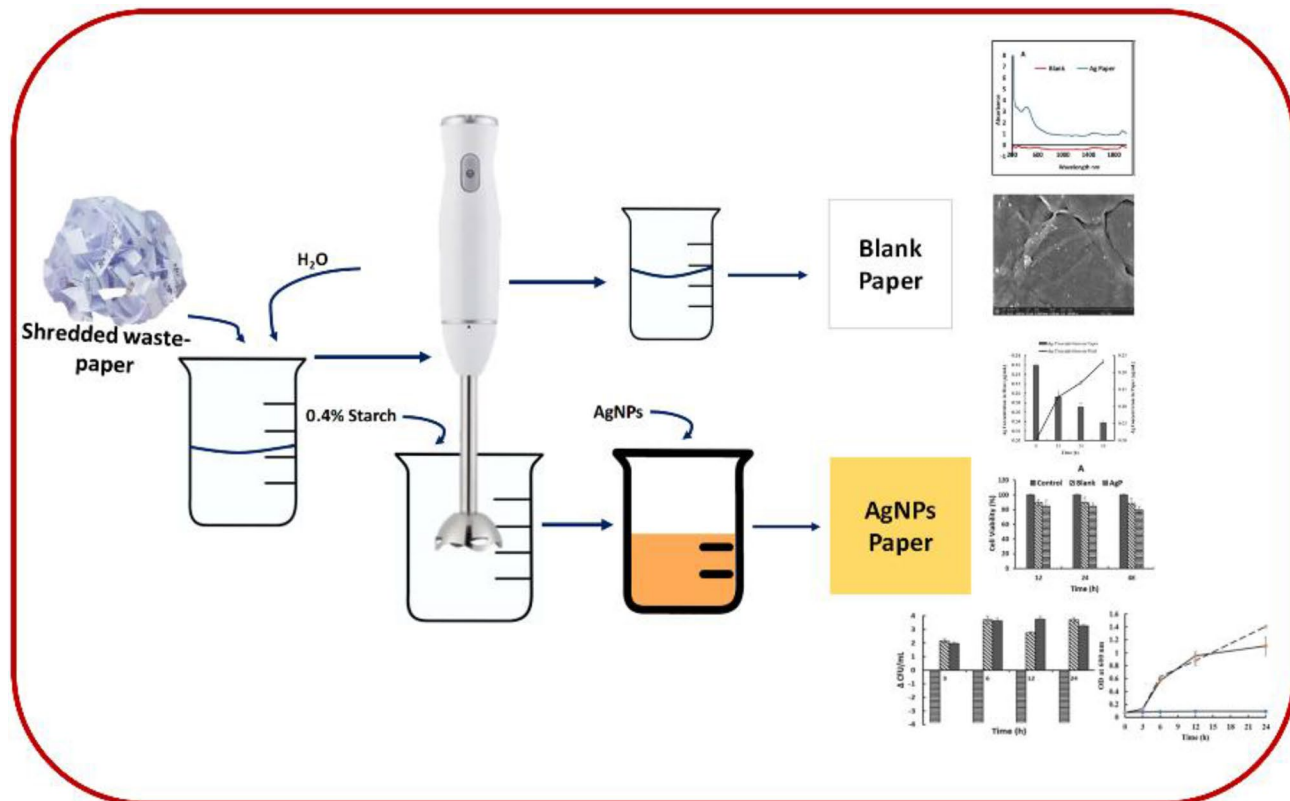
¹ Division of Infectious Diseases, Department of Internal Medicine, Faculty of Medicine, Prince of Songkla University, Hat Yai, Songkhla 90112, Thailand

² Excellence Research Laboratory on Natural Products, Division of Biological Science, Faculty of Science and Natural Product Research Center of Excellence, Prince of Songkla University, Hat Yai, Songkhla 90112, Thailand

³ Cosmetic Technology and Dietary Supplement Products Program, Faculty of Agro and Bio Industry, Thaksin University, Ban Pa Phayom, Phatthalung 93210, Thailand

⁴ Department of Food Technology, Faculty of Agro-Industry, Prince of Songkla University, Songkhla 90112, Thailand

Graphic Abstract



Keywords Valorization · Recycled wastepaper · Functionalization · Nanocomposite · Antimicrobial · Packaging material

Statement of Novelty

The current work provides a novel and cheap process for the recycling and reuse of paper, which can be used as packaging material. Biogenic silver nanoparticles synthesized from waste plant material served as active agent. The nanocomposite paper demonstrated good antibacterial activity. The work demonstrated that functionalized recycled paper could be an alternative inexpensive packaging material.

Introduction

Paper and paper-based materials are excellent consumer products extensively used in packaging, sanitary products, and stationaries. They are described as green packaging materials due to their renewability, recycling, and biodegradability [1]. Unfortunately, in most developing and underdeveloped nations, paper-based products serve for single usage thus contributing to the bulk of municipal solid waste generation.

About 2.01 billion tonnes of municipal solid waste were generated globally in 2016, and the figures are expected to increase to 3.40 billion tonnes by 2050 [2]. Global solid waste composition indicates that waste papers and cardboards constitutes 17% of the total municipal solid waste generation [2]. Although papers and paper-based products are generally biodegradable, they deform environmental aesthetics. Moreover, wood pulping for paper production results tree falling, leading to deforestation, global warming and desertification. Approximately 4 billion trees worldwide are lost annually to paper production, representing 35% of all harvested trees. This figure is critical to deforestation and other severe environmental outcomes like drought and desertification [3].

Recovery and recycling of waste is an emerging market with prospective applications in developing and underdeveloped countries [4, 5]. Recycled paper presents a cheap, renewable and sustainable source of material that can be used in the fabrication of packaging material. However, for safety reasons, it is important that such papers be fortified and functionalized for maximum product.

Functionalization of waste has been reported as a sustainable environmental approach [6].

Microbial spoilage and deterioration are global problems resulting in the loss of agricultural produce and industrial finished products. It is estimated that 1.3 billion tons of agricultural products are lost annually to spoilage [7], with about 25% lost due to microbial spoilage [8]. Efforts at controlling the menace posed by spoilage microorganisms, has birthed several novel strategies in the design of packaging materials. Smart, intelligent and active packaging materials through the incorporation of bioactive agents into carriers such as polymers have dominated the research domain. However, most polymers are expensive and often lack required properties for an ideal packaging material.

In this study, bioactive ethanolic leaf extracts of *Eucalyptus camaldulensis* [9–11] was used as reducing and capping agent in the synthesis of biogenic silver nanoparticles. Wastepaper collected from paper bin were recycled and functionalized with silver nanoparticles. The biogenic silver nanoparticles and bioactive paper were characterized and evaluated for antimicrobial activities against important foodborne pathogenic bacteria. In addition, the release and migration of silver and toxicity of the released silver to human cell lines were monitored.

Materials and Methods

Materials

Silver nitrate and starch were purchased from Sigma Aldrich, Singapore. Ethylene Tetrazolium Bromide (3-(4,5-dimethyl-2-thiazolyl)-2,5-diphenyl-2H, MTT), and trypsin were purchased from Merck. Dulbecco's modified eagle medium (DMEM) and fetal bovine serum were purchased from Gibco, UK.

Plant Material and Extraction

Classified reference voucher specimen of *E. camaldulensis* was deposited at the Herbarium of Faculty of Pharmaceutical Sciences, Prince of Songkla University, Thailand. The leaves were extracted by maceration methods using 95% ethanol as solvent.

Silver Nanoparticles Synthesis

Ethanolic leaf extract of *E. camaldulensis* (20 mg/mL) was solubilized with dimethyl sulfoxide. Subsequently, 1 mL of the extract was added into 120 mL of deionized water to a final concentration of 0.167 µg/mL. Anhydrous AgNO₃ was dissolved in deionized water (~21.5 mg/mL), and 1 mL was added to the solution containing extract at a final

concentration of 179 µg/mL. The mixture was left stirring for 40 min at room temperature until a deep brown colouration indicating reduction of the silver salt. The Silver nanoparticles solution was centrifuged at 12,000 rpm for 30 min, and the supernatant was decanted. Pellets were resuspended in deionized water and stored in the dark.

Antimicrobial Activities of Silver Nanoparticles

The antibacterial effects of the green synthesized silver nanoparticles was determined using the standard broth microdilution method [12]. In brief, the bacterial cells were grown to log phase (4–5 h) in Mueller-Hinton Broth. The cells were then adjusted to a final concentration of 10⁶ CFU/mL, and 100 µL of cell suspension was added to serially diluted AgNPs concentrations in 96 well micro-titre plates and incubated at 37 °C overnight. The MIC values were recorded as the lowest concentration that completely inhibited the bacteria growth, and the minimum bactericidal concentration (MBC) values as the lowest concentrations that showed no growth on tryptic soy agar (TSA) plates after incubation for 24 h. All the experiments were set up in triplicates for two independent studies. *Escherichia coli* O157:H7, *Listeria monocytogenes* F2365, *Staphylococcus aureus* ATCC 25,923 and an isolate of *Bacillus cereus* were used in the assay.

Evaluation of Potassium Ions Leakage from Bacterial Isolates

The membrane disruption activities of the biogenic silver nanoparticles were estimated by measuring the potassium ion concentration released from the bacterial pathogens into the surrounding medium. Exponential phase bacterial cultures were harvested at 4500 rpm for 5 min and resuspended into PBS (pH 7.4). The bacterial suspensions were treated with bactericidal concentrations of silver nanoparticles and incubated for 4 h. Untreated bacterial suspensions were used as negative control. The bacterial suspensions were centrifuged at 8000 rpm for 10 min and the supernatant collected. The leakage of K⁺ from the cells was measured using inductively coupled plasma-optical emission spectroscopy (ICP-OES, Optima 8000, Perkin Elmer, MA, USA).

Effects of Silver Nanoparticles of Cell Membrane of Foodborne Pathogens

The effects of the silver nanoparticles on the cell membrane of foodborne pathogenic bacterial isolates was investigated by scanning electron microscopy. Overnight bacterial cultures were harvested at 4500 rpm for 5 min and adjusted using a spectrophotometer to optical density of 0.2 at 600 nm. The cultures were treated with fourfold

minimum inhibitory concentrations of silver nanoparticles (3.98–7.92 µg/mL) and incubated at 37 °C for 4 h. The cells were washed with normal saline and aliquot spotted on a 1 cm² glass slide. Dried cells on glass slide were fixed in 3% (v/v) glutaraldehyde for 2 h and serially dehydrated using 20, 40, 60, 80, and 100% ethanol for 15 min each. Morphology of the bacterial cells was examined under a scanning electron microscope (Quanta 400 FEI, Oregon, USA).

Characterization of Silver Nanoparticles

Preliminary confirmation of silver nanoparticles synthesis was detected using UV–visible spectroscopy at a wavelength of 300–800 nm (2300 EnSpire, multimode plate reader, Perkin Elmer, USA). Fourier transform infrared (FTIR) (VERTX 70, Bruker, Germany), scanning electron microscopy (SEM) and transmission electron microscopy (TEM-Hitachi, Tokyo, Japan) were performed to study the molecular interactions, shape, and size of the silver nanoparticles. Zeta potential and size of synthesized NPs were measured using zeta PALS-zeta potential analyzer by dynamic light scattering (DLS). Elemental composition of silver nanoparticles was analyzed by an energy dispersive X-ray spectroscopy (EDX) coupled to field-emission scanning electron microscope (FESEM).

Wastepaper Recycling and Nanocomposite Paper Fabrication

Shredded pieces of papers of weight 4.45–5.00 g, equivalent to an A4 paper were sterilized under UV. The paper was then blended into pulp in 500 mL of distilled water using an Electrolux blender Model No. ESTM54175, China with 0.4% starch added as binder. The nanocomposite paper was fabricated by blending in 400 mL of distilled water and 100 mL of 0.163 µg/mL colloidal silver nanoparticles solution. The mixtures were heated in a microwave for 5 min at a temperature of 80–90 °C. Afterwards, 250 mL portion of each mixture was casted on a tray covered with muslin cloth in a 19.5 × 28 cm frame. The casted pulp was left to drain water and was then transferred to an oven (70 °C) to dry for 6 h.

Characterization of Active Nanocomposite Paper

The fabricated nano composite paper and blank were characterized for physicochemical, mechanical, structural and functional properties using various techniques as described below.

Fourier Transformed Infrared Spectroscopy (FTIR)

Chemical structures of the recycled nanocomposite paper and blank control paper were analysed by attenuated total

reflectance Fourier-transform infrared (ATR-FTIR) spectrometry with resolution of 4 cm⁻¹, aperture setting of 6 mm and scanner velocity of 2.2 kHz. The spectral were acquired at 4000–500 cm⁻¹ by Bruker 66 spectrometer (Germany).

X-ray Diffraction (XRD)

The X-Ray diffraction pattern of the samples were obtained with a reference target of Cu K α radiation (the weighted average $\lambda = 0.15406$ nm) voltage of 40 kV, current of 30 mA. The samples were measured at an angle of 2θ with steps of 0.026° (2θ)/min at time 70.125 sec/step using (Empyrean, PANalytical, Netherlands).

Scanning Electron Microscope (SEM) and Energy Dispersive X-ray (EDX)

The morphology of synthesized nanocomposite paper and blank recycled paper were examined by Field emission scanning electron microscopy (SEM, Quanta 250 SEM-FEI, FEI/Thermo Fisher Scientific, USA). Piece of sample was mounted on an aluminium stub and sputter-coated with gold. The elemental compositions of the samples were also obtained by EDS analysis (EDS, JEOL, JSM-6010LA). In addition, mapping for the distribution of elemental components was done using EDS technique.

Thickness and Tensile Strength

Nano composite paper thickness was measured by a digital micrometer (Mitutoyo Manufacturing Co. Ltd., Tokyo, Japan) and recorded as mean value in micrometer (mm) \pm SD. The tensile strength (TS), and percentage elongation at break (EAB) were evaluated using tensile testing machine, Zwick Roell Germany (Z010). Five dumb-bell shaped samples of 115 mm length and 20 mm width were analysed for each film. Films were mounted on the film extension grip at an initial grip distance of 50 mm and crosshead speed was 50 mm/min. Tensile strength, elongation at break, and Young's modulus were obtained from the testXpert® II software version 3.31 that comes with the instrument.

Grammage and Bulk Density Analysis

Synthesized silver nanoparticles and blank recycled paper were cut into 10 cm × 10 cm and weighed using an analytical balance to give the response in g/m². The bulk density of the samples were calculated according to ISO 534 from the ratio between the grammage and thickness [1].

Water Absorption

Water absorption capacity of the recycled nanocomposite paper and blank control was determined after 24 h immersion in water using $2 \times 2 \text{ cm}^2$ piece of each sample. The initial dry weight (M_{dry}) of the samples was recorded, afterward the samples were placed in a petri dish containing 10 mL of distilled water. After 24 h, the excessive water was wiped off with blotting paper. The wet dry weight (M_{wet}) of the samples were measured and the water absorption capacity was calculated and recoded in (g/m^2).

$$WA (\%) = \frac{[M_{wet} - M_{dry}]}{M_{wet}} \times 100 \quad (1)$$

UV–Visible Spectroscopy

The nano composite and blank control paper were characterized by UV–visible spectroscopy analysis. The absorbance and percentage reflectance from synthesized nanocomposite papers and blank were measured for wavelengths between 200 and 1800 nm using a UV–vis spectroscopy (F300s Ultraviolet lamp, Shimadu, Tokyo).

Silver Release and Migration in Minced Meat

To study the migration of silver from synthesized nanocomposite paper into the meat, the papers were cut into circles of diameter 5 cm. Then, 5 g of minced meat was weighed into a petri-dish of diameter (5 cm) and flattened to form a bed with uniform surface. Synthesized nanocomposite paper was placed on the surface of the meat such that the entire surface was in contact with the meat. The paper surface was damped with 500 μL of distilled water to act as a mobilizer and plates were stored at refrigerator temperature 4–7 °C. At 0, 12, 24, and 48 h paper samples were carefully removed from the meat surface and analysed for silver content using Inductively coupled plasma–optical emission spectrometry (ICP–OES). The concentration of silver that has migrated into the meat was calculated as the difference between the paper silver content at a given time and the silver content at time 0 h.

Release Models

To further study the pattern of Ag release from the recycle nanocomposite paper, the In vitro release data were fitted into various kinetic models like zero-order, first order, Higuchi, and Korsmeyer–Peppas's, equation and coefficient

of correlation (r) values were calculated for linear curves by regression analysis of the plots.

Cytotoxicity of Silver Nanoparticles Packaging Paper

Synthesized nanocomposite paper was evaluated for toxicity using HEK293T and Caco-2 human cell lines as described [13] with modifications. The cells were collected from the Department of Physiology, Prince of Songkla University and cultured in high glucose DMEM supplemented with 10% fetal bovine serum (FBS) and 1% penicillin–streptomycin solution. Approximately 1×10^4 cells were seeded in 96-well plates (100 μL /well) and incubated at 37 °C in an incubator humidified with 5% CO_2 atmosphere for 24 h. The medium was removed, and the cells were washed twice with phosphate buffer solution. The cells were exposed to 100 μL of medium containing silver nanoparticles released from the packaging material at different time intervals (12, 24, and 48 h). Release media from recycled control paper and fresh media were used as control. The cells were then incubated for 24 h in a CO_2 incubator at 37 °C. Cell viability after exposure to treatment, blank and control was analyzed using MTT assay Briefly, 10 μL of 5 mg/mL MTT solution in PBS buffer and 100 μL of DMEM was added to each well and incubated in the dark for 4 h. The absorbance (optical density) value of the wells was measured at a wavelength of 570 nm using a multi-mode plate reader Enspire. The percentage cell viability was then calculated as

$$\frac{OD_{Treatment}}{OD_{Control}} \times 100 \quad (2)$$

In Vitro Antimicrobial Activities of Active Paper

The nanocomposite paper and blank were tested for antibacterial activities against important Gram-positive and Gram-negative foodborne pathogenic bacteria including *L. monocytogenes* F2365, *S. aureus* ATCC 25,923, an isolate of *B. cereus* and *E. coli* O157.H7. The bacteria cultures were incubated at 37 °C overnight in Muller Hinton broth (MHB). The culture was harvested and adjusted to 10^6 CFU/mL before use. The method of [14] was adopted in a 24 well plate with slight modifications using piece of paper (3 cm^2) in 1.5 mL of bacterial suspension. The plates were incubated statically at 37 °C, and aliquot of samples were withdrawn, plated out on TSA and counted at 3, 6, 12, and 24 h. Samples were also prepared for OD measurement at each of the test time. OD values were recorded at 600 nm and change in bacterial population as $\Delta\text{CFU}/\text{mL}$.

Antibacterial Testing (ISO 20743)

The survival of bacterial isolates in contact with synthesized silver nanoparticles packaging paper was evaluated using a modified method from ISO 20743. The test bacterial isolates and strain were maintained in tryptic soy broth to exponential growth phase and used for the testing. Briefly, the cultures were diluted in TSB to 1.5×10^8 CFU/mL. Then 50 μ L of the diluted bacterial suspension was loaded onto synthesized nanocomposite paper and blank control. The test papers were left damp and then incubated in a humid condition for 24 h. Afterwards, the surviving bacterial on the papers were enumerated in 1 mL of neutralizer solution and serial dilution using saline solution. Aliquot (10 μ L) of the dilutions were spot plated on TSA and incubated overnight at 37 °C. Bacterial colonies were then counted and recorded as CFU/mL.

Statistical Analysis

All experiments were performed in triplicate for two independent studies. The results were statistically analysed using analysis of variance. Data were tested using the Scheffe statistical test (SPSS 20). A 95% confidence limit ($p < 0.05$) was adopted throughout the study.

Results and Discussion

Synthesis and Characterization of Biogenic Silver Nanoparticles

Reduction of metal salts with plant extracts and phytochemicals has been described as an eco-friendly alternative method for the synthesis of NPs with excellent bioactive properties. Ethanolic extracts of *E. camaldulensis* was successfully used as a reducing and capping agent for AgNO_3 . The formation of silver nanoparticles was signalled by colour change and confirmed using UV–visible spectroscopy (Fig. 1a). The

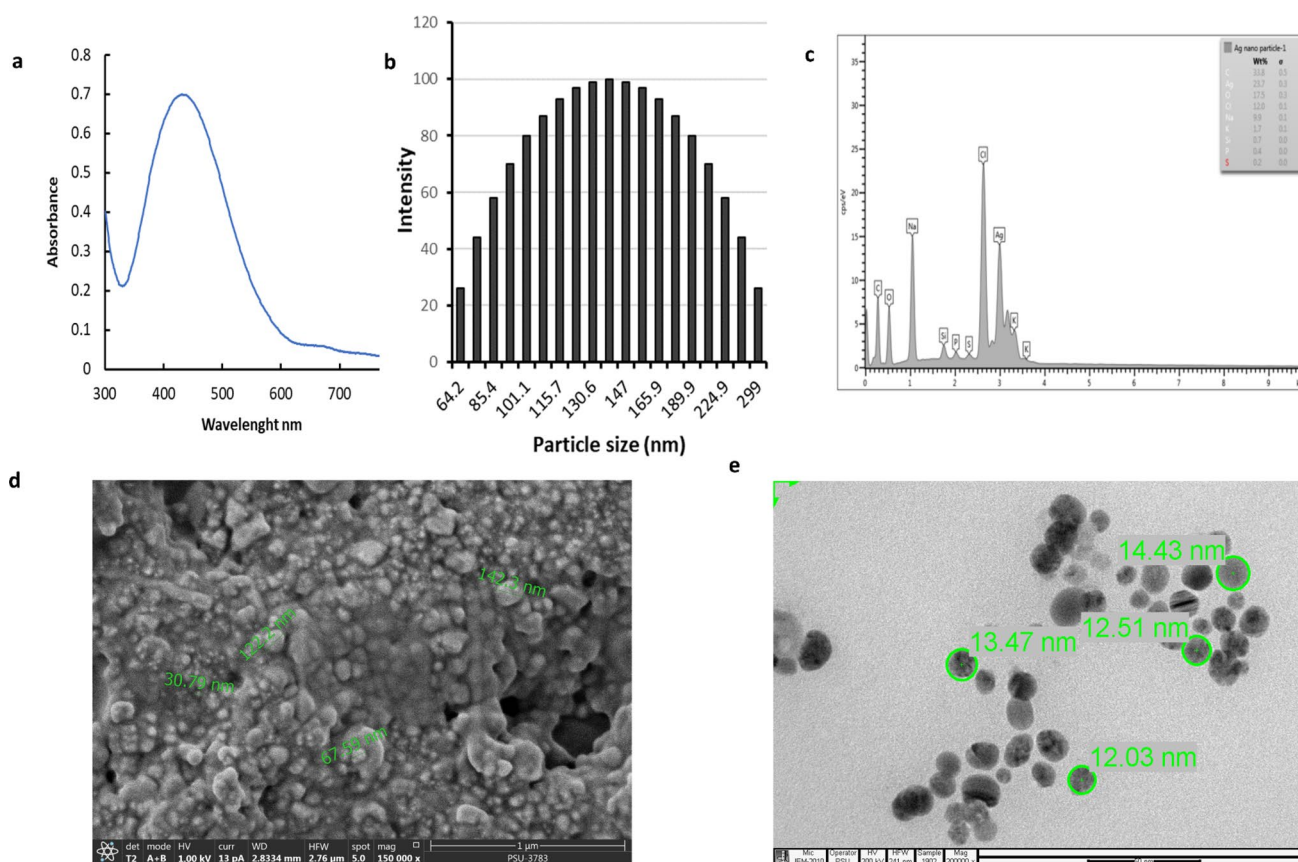


Fig. 1 Characterization of biogenic silver nanoparticles using UV-visible spectroscopy (a) showing the Ag plasmon resonance peak at 437 nm, Dynamic light scattering (b) showing particles size distribution of the, Energy dispersive X-ray spectroscopy (c) showing

the elemental components of the silver nanoparticles with a silver concentration of 23.7%Wt, Scanning electron (d), and transmission electron micrographs (e) showing spherical particles and size of the nanoparticles

peak at 437 nm represented the surface plasmon resonance of silver nanoparticles. DLS analysis showed that the silver nanoparticles had an effective diameter of 138.6 nm with a polydispersity of 0.244 (Fig. 1b) and (Fig. S1), and zeta potential of -35.85 mV (Fig. S2). The high negative zeta potentials indicate high stability of the silver nanoparticles due to electrostatic repulsive force [15]. Elemental analysis of the silver nanoparticles by EDX indicated Ag concentration of 23.7%Wt (Fig. 1c). Furthermore, visualization of the NPs by SEM and TEM (Fig. 1d and e) showed clusters of spherical shaped nano-sized particles.

Antimicrobial Activities of Biogenic Silver Nanoparticles on Foodborne Pathogens

Plant synthesized silver nanoparticles have demonstrated a broad-spectrum antimicrobial activity against various foodborne pathogenic and spoilage microorganisms. In this study, the synthesized silver nanoparticles exhibited good bactericidal activities against foodborne pathogenic bacteria, including *B. cereus*, *E. coli*, *L. monocytogenes* and *S. aureus* (Table 1). The minimum inhibitory concentrations and the minimum bactericidal concentrations ranged from 0.99 to 1.99 and 3.98–15.91 $\mu\text{g/mL}$ respectively. Similar findings have earlier been reported [16]. Although the antimicrobial properties of silver nanoparticles have been extensively explored, the exact mechanism of action is still not fully elaborated. However, the antimicrobial effects of silver nanoparticles is dependent on factors including the size, morphology, physicochemical properties of the silver nanoparticles as well as the culture medium, microbial environment, and method of synthesis [17].

Potassium Ion Leakage

Bacterial plasma membrane constitutes a permeable barrier that regulates the movements of molecules in and out of the cell cytoplasm. Thus, alterations and poration of the plasma membrane by antimicrobial agents results in the loss of functionality leading to increased efflux of important cellular electrolytes that are required for proper cell functions. The membrane disruption activities of biogenic silver nanoparticles evaluated by potassium leakage is presented in (Fig. S3). The results indicated silver nanoparticles concentration

dependent K^+ release. Increase in the K^+ leakage after treatment with silver nanoparticles suggest an increase in the efflux of important ions from the cell and might be due to structural and functional alterations of the membrane by the silver nanoparticles or formation of pores on the plasma membrane. The results further suggested low K^+ release from *S. aureus*, this might be to the difference in MBC value observed.

Silver Nanoparticles Mediated Membrane Rupture

The disruptive effects of the silver nanoparticles on the cell membrane of pathogenic foodborne isolates and strains were confirmed by scanning electron microscopy (Fig. 2). The micrograph presented intact and healthy cell membrane for untreated control cells, whereas silver nanoparticles treated cells were observed to exhibit extensive membrane damage with structural deformation, poration and shrinkage. Bacterial cell membrane plays an important role as selective permeable barrier. Disruption of the cell membrane due to treatment with silver nanoparticles alters the membrane functionality, resulting in the influx of extracellular molecules into the cell, leading to lysis of the cell. The micrograph confirms that silver nanoparticles exerts its antibacterial effects by disrupting the cell membrane of the cell and thus enhancing the influx and efflux of extracellular materials and intracellular components, respectively. Similar results have been previously reported [18, 19]. In addition, alteration of redox homeostasis and induction of oxidative stress are reported as possible route of silver nanoparticles antimicrobial mechanism [20, 21].

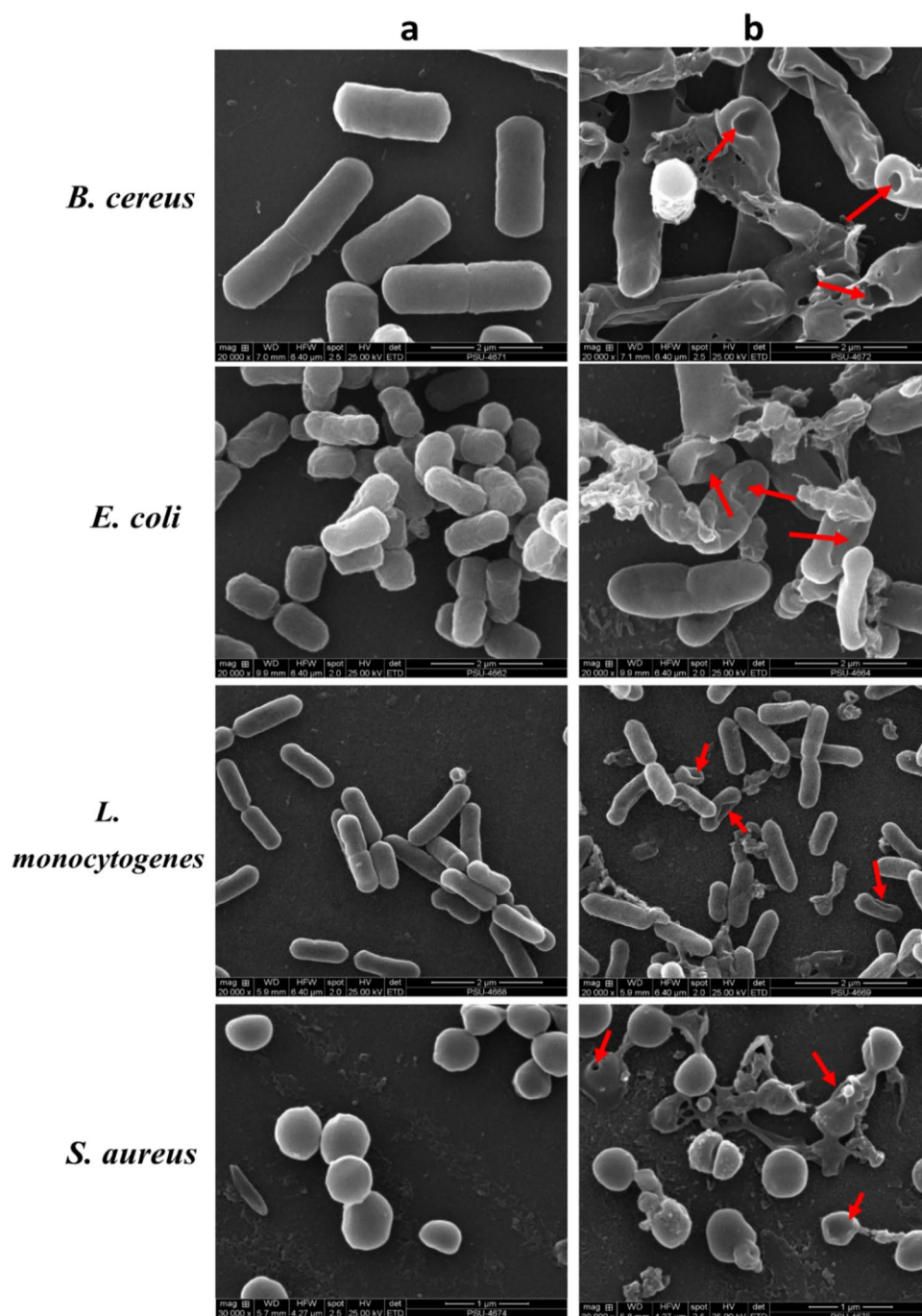
FTIR Analysis

The FTIR spectra of the biogenic silver nanoparticles, extract, recycled control, and synthesized nanocomposite paper is presented in (Fig. 3a). Synthesized silver nanoparticles and ethanolic extract of *E. camaldulensis* spectra showed a broad band between 3400 and 3450 cm^{-1} representing the O–H stretching vibration of the phenolic and flavonoid compounds. Peak at 2920–2925 cm^{-1} is ascribed to the $-\text{CH}_2$ and C–H stretching of alkanes. The prominent peaks at 1620–1640 cm^{-1} reflects the N–H presence of amine group. The extract and silver nanoparticles

Table 1 Antibacterial activities of silver nanoparticles against pathogenic foodborne bacterial isolates evaluated using micro-broth dilution assay

Isolates	Minimum inhibitory concentrations ($\mu\text{g/mL}$)	Minimum bactericidal concentrations ($\mu\text{g/mL}$)
<i>Bacillus cereus</i>	0.99	3.98
<i>Escherichia coli</i> O157:H7	1.99	3.98
<i>Listeria monocytogenes</i> F2365	1.99	7.96
<i>Staphylococcus aureus</i> (ATCC 25,923)	1.99	15.91

Fig. 2 Scanning electron micrograph of silver nanoparticles treated foodborne bacterial isolates. Showing rupture, poration and damage of bacterial cell membrane after treatment with bactericidal concentrations of silver nanoparticles for 4 h



spectra displayed visible interaction between functional groups. The absence of the aliphatic saturated aldehydes carbonyl group $C=O$ ($1690\text{--}1750\text{ cm}^{-1}$) observed in the extract, merging of the multiple weak bands of polyols $C-O$, alkanes $C-H$ and $C-H$ deformation vibrations ($1190\text{--}1450\text{ cm}^{-1}$) present in the extract into a single sharp and prominent peak at 1384 cm^{-1} and shift of $-C-O-$ stretching of alcohols, carboxylic acids, esters and ethers from 1045 to 1115 cm^{-1} indicates the reduction of Ag^+ ions by plant phytochemicals or adsorption of

phytochemical compounds from the extracts onto the nanoparticle surface [22]. The FTIR spectra of the recycled control paper and nanocomposite paper displayed similar peaks, with minor peak shifts at 3331 to 3329 , 2898 to 2900 , 1726 to 1722 , 1639 to 1637 , 1426 to 1413 , 1023 to 1021 . The absence of major changes in the functional groups is attributed to the usage of an already reduced Ag^+ . Previous researchers have demonstrated slight alterations in the functional groups of cellulose paper following the reduction of $AgNO_3$ [23, 24].

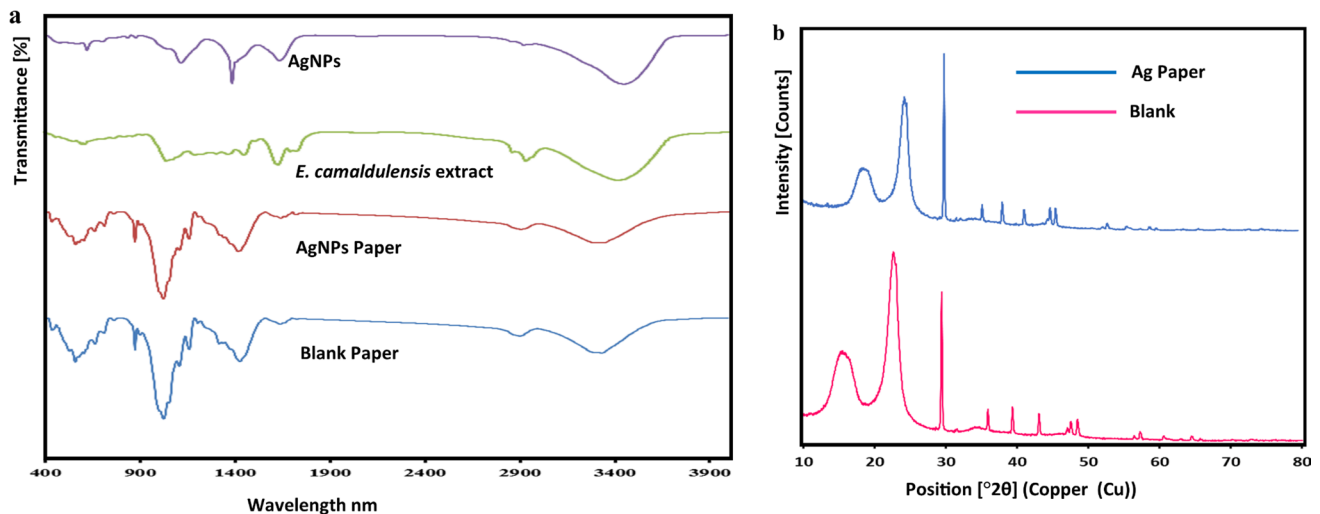


Fig. 3 FTIR spectra of silver nanoparticles, *E. camaldulensis* extracts, nanocomposite and recycled control paper showing the functional groups present in the samples and the chemical interactions between functional groups (a), and XRD spectra of the nanocompos-

ite and recycled control paper indicating the absence of silver peaks due to the low concentration of Ag lower than the 2% dictation limit (b)

XRD Analysis

The XRD spectra presented in (Fig. 3b) showed that both blank control and nanocomposite paper presented similar amorphous to crystalline peaks. The XRD peaks at $2\theta = 16.5^\circ$, 22.6° , and 22.9° were ascribed to (1–10), (110), and (200) planes of cellulose II crystalline structure [25, 26]. Additional peaks in synthesized nanocomposite paper at $2\theta = 32.2^\circ$ and 77.3° were attributed to (111) and (311) crystal planes of face centred cubic structure of silver [27]. The intensity of peaks of recycled control paper were also observed to be higher than those of synthesized nanocomposite paper, indicating a lowering of crystallinity by the presence of Ag nanoparticles [27]. This confirms the physical interaction of synthesized silver nanoparticles with component compound of cellulose paper.

UV–visible Spectra of Recycled Nanocomposite Paper

The absorbance and reflectance spectra of composite papers were recorded at wavelengths between 200 and 2000 nm (Fig. 4a). The absorbance spectra of synthesized nanocomposite paper showed a peak at 427 nm resulting in a downward trough in the reflectance spectra (Fig. 4b). This represents the plasmon resonance band of synthesized silver nanoparticles. The narrow width of the peak suggests a narrow size distribution of synthesized silver nanoparticles present in the paper. At the wavelength range tested, recycled control paper consistently presented a higher reflectance, whereas synthesized nanocomposite paper showed higher

absorbance. This indicates the colour alteration witnessed with synthesized nanocomposite paper. The recycled control paper reflected all light wavelength whereas the deep brown colour of synthesized silver nanoparticles absorbed the light. Previous researchers have reported reduced light reflectance of paper after incorporation of silver nanoparticles [28, 29]. silver nanoparticles have also been reported to exert a UV blocking activity [30], and capable of absorbing a wide wavelength range of lights [31]. These unique properties of silver nanoparticles define its optical application in various fields.

Physicochemical Parameters of Recycled Paper

The physicochemical and mechanical properties of recycled paper are presented in (Table 2). The tensile strength of a material reflects the ability to resist breaking under stress and is dependent on the strength of the base material, surface area, length, and the bonding strength between them. Whereas the elongation at break shows the ability of a material to stretch before breaking. The results obtained reveals that synthesized nanocomposite paper showed significant increase in tensile strength ($p < 0.05$) compared to blank control. However, the percent elongation at break was significantly higher for recycled control paper. The increased tensile strength might be due to the formation of strong bonding between the paper base material and synthesized silver nanoparticles. Similar results were obtained following reinforcement of active nanocomposite pouches with in situ generated silver nanoparticles [32]. The thickness of the recycled

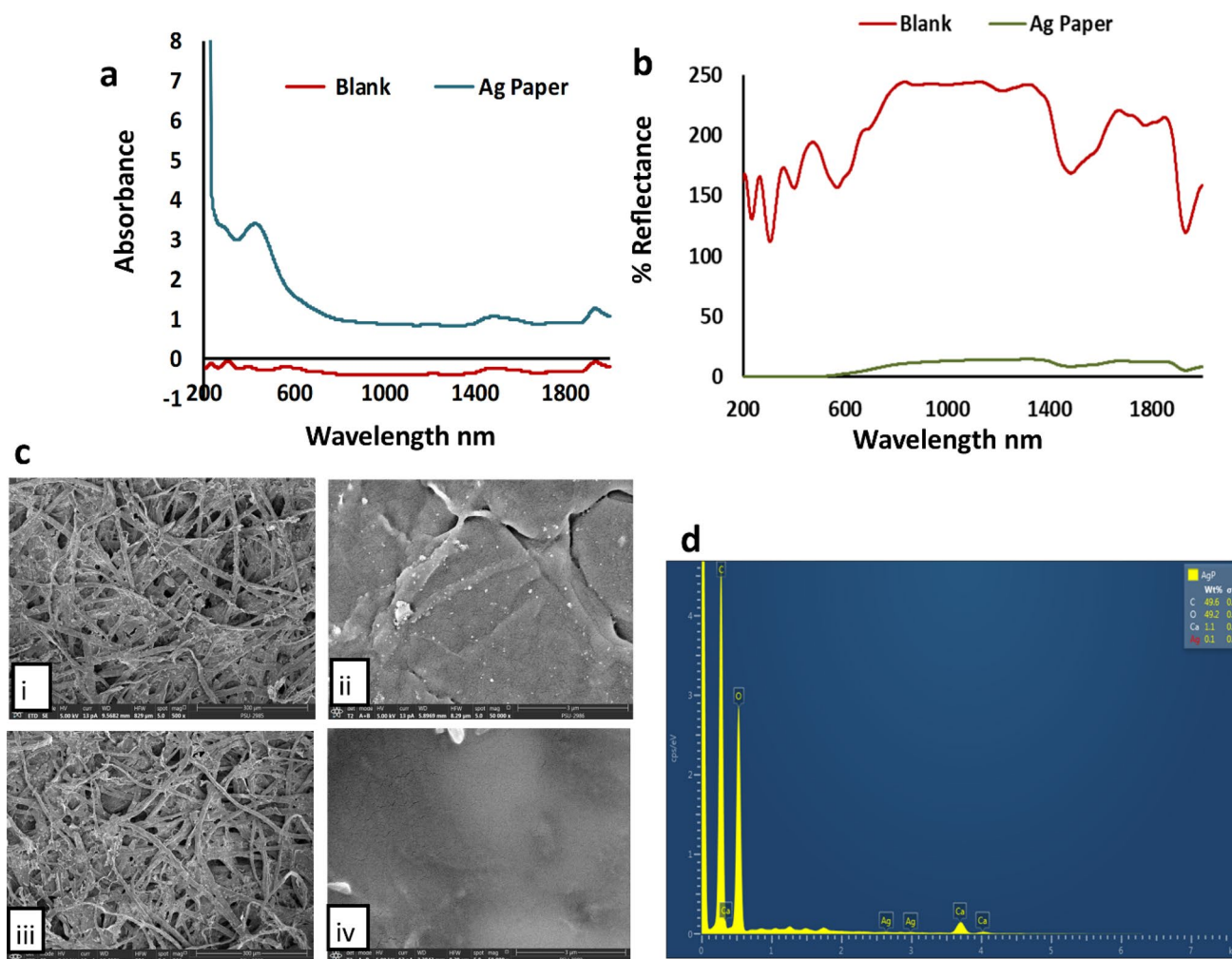


Fig. 4 Optical properties of silver nanoparticles paper showing (a) absorbance spectra with surface plasmon resonance peak of silver nanoparticles at 427 (b) reflectance spectra, (c) scanning electron micrograph of nanocomposite paper, (i) and (ii) shows the structure

and nanoparticles dispersion on the nanocomposite paper while (iii) and (iv) shows structure and plain surface of control paper, (d) EDX spectra showing the Ag^+ content of the nanocomposite paper in Wt%

Table 2 Mechanical and physicochemical characteristics of the nanocomposite and recycled control papers

Samples	T_{\max} (MPa)	EAB (%)	Thickness (mm)	Water absorption (g/m^2)	Grammage (g/m^2)	Bulk density (g/cm^3)
Ag Paper	5.8 ± 0.71^a	0.7 ± 0.34^a	0.18 ± 0.01^b	57.7 ± 2.29^b	87.4 ± 0.9^b	0.49 ± 0.02^b
Blank	3.7 ± 0.67^a	1.6 ± 0.36^a	0.19 ± 0.01^b	60.1 ± 1.99^b	90.4 ± 1.4^b	0.48 ± 0.03^b

^aSignificant different

^bNot significantly different ($p < 0.05$)

paper ranged between 0.18 and 0.19 mm. No significant difference ($p < 0.05$) was observed in the physicochemical parameters (water absorption, grammage, and bulk density of the samples) of synthesized nanocomposite paper and the blank.

Scanning Electron Micrograph of Recycled Nanocomposite Paper

The morphology of the recycled nanocomposite paper and blank control is shown in (Fig. 4c). The surface micrograph

of the samples as shown by SEM revealed a cellulose base fibrous net-like structure. However, unlike the image previously reported, incorporation of silver nanoparticles into the paper did not affect the surface pore size of the paper [33, 34]. The difference might have resulted from the coating method employed by the previous researchers. At higher magnifications, the nanocomposite paper reveals spherical nanosized particles distributed on the surface which are believed to be silver nanoparticles embedded on the surface of the paper (Fig. 4cii). On the contrary, the recycled control papers at same magnification revealed a smooth surface, showing the absence of particles. To confirm the presence of synthesized silver nanoparticles on the paper, EDX elemental analysis was performed on synthesized silver nanoparticles functionalized paper (Fig. 4d). The EDX quantitative revealed Ag concentration of 0.1%Wt on the paper. Mapping of the paper surface further showed uniform distribution of synthesized silver nanoparticles on the surface of the paper. Other elemental components of the paper included carbon and oxygen from the cellulose base and starch added as binder and calcium probably from CaCO_3 serving as filling material in the paper production (Fig. S4).

Release and Migration of Ag from Synthesized Nanocomposite Paper

To investigate the release profile of Ag from synthesized silver nanoparticles packaging paper and migration into wrapped food, a food model-based method was developed using minced beef. The initial concentration of Ag and Ag release at various intervals was evaluated using ICP-OES (Fig. 5a). The results obtained revealed an initial Ag concentration of 0.22 $\mu\text{g/mL}$. After 12 h, 41.8% of the Ag content was reduced, indicating migration from the packing paper into the minced meat product. At 48 h, approximately 75.9% of the Ag was migrated into the meat. The result demonstrates an unregulated release of silver. Similar result was observed by [35] who reported a high Ag^+ release from bacterial cellulose/silver nanoparticles composite within 72 h. The antimicrobial activity of silver nanoparticles has been demonstrated by various researchers, however the easily leakage of silver from composite materials restricts its application in the design of packaging materials [36]. Cytotoxicity of silver nanoparticles to cells has also been attributed to this uncontrolled release, regulating the release of Ag from composite material reduces the cytotoxicity to cells [36].

The release kinetics of Ag from the recycle nanocomposite paper showed “r” value of (0.978) for first order kinetics indicating a concentration dependent In vitro release. The interpretation of release exponent values (n) was studied to understand release mechanism of silver nanoparticles from the recycled nanocomposite paper. The Higuchi and Korsmeyer-Peppas model presented a linearity of 0.996 and

0.986 for silver nanoparticles, whereas Peppas’s model suggests classic Fickian diffusion with n values of 0.434.

Cytotoxicity of Nanocomposite Paper

The effects of silver nanoparticles and its toxicity on the environment and humans has attracted great attention due to the growing interest in silver nanoparticles and its applications in various area including consumer goods. Thus, to validate the use of silver nanoparticles as active agents in the design of food packaging materials, antimicrobial nanocomposite paper and blank control paper were evaluated for toxicity against human renal cell HEK293T and human colon cell line Caco-2 (Fig. 5b). The result showed that silver nanoparticles at the concentrations released after 12, 24, and 48 h showed no toxicity against both cell-lines. The human renal cell HEK 293T showed approximately $\geq 80\%$ viability (i), whereas Caco-2 cells showed $> 90\%$ viability (ii) at all the tested time. Silver nanoparticles has been previously reported to exhibit a mild toxic effect on HEK 293T at a high concentration of 20 $\mu\text{g/mL}$ [13]. On Caco-2 cells, silver nanoparticles has been reported to exert a non-toxic effect on differentiated Caco-2 cells at concentrations $\leq 50 \mu\text{g/mL}$ [37]. The effects of silver nanoparticles is dependant of various factors such as the size of the nanoparticles, concentration, time of exposure [38]. The non-toxic effect of silver nanoparticles observed in this research could be as a result of the low concentration of Ag and incomplete release of all the silver content of the paper. At all tested time, the recycled control paper also showed no toxic effects on HEK 293T, and in addition tends to show stimulatory effects on Caco-2 cells.

Antibacterial Potency of Synthesized Nanocomposite Paper

The antibacterial effects of synthesized silver nanoparticles and blank control paper were demonstrated against food-borne pathogenic bacterial isolates including *B. cereus*, *E. coli* O157:H7, *L. monocytogenes* F2365, and *S. aureus* ATCC 25,923 in a broth culture base method (Fig. 6). The results showed pronounced bactericidal effects on *B. cereus* and *E. coli* with $> 3\log$ reduction after 3 h of treatment. Against *L. monocytogenes* and *S. aureus*, the paper showed bacteriostatic effects with approximately 1log reduction after 12 h treatment. The antimicrobial effects of the blank control paper were like that of bacterial culture without a test paper. This indicates that the antimicrobial observed with synthesized nanocomposite paper was as a result of the Ag released from synthesized nanocomposite paper into the broth culture. The antimicrobial effects of silver nanoparticles coated cellulose paper has been previously demonstrated [39, 40].

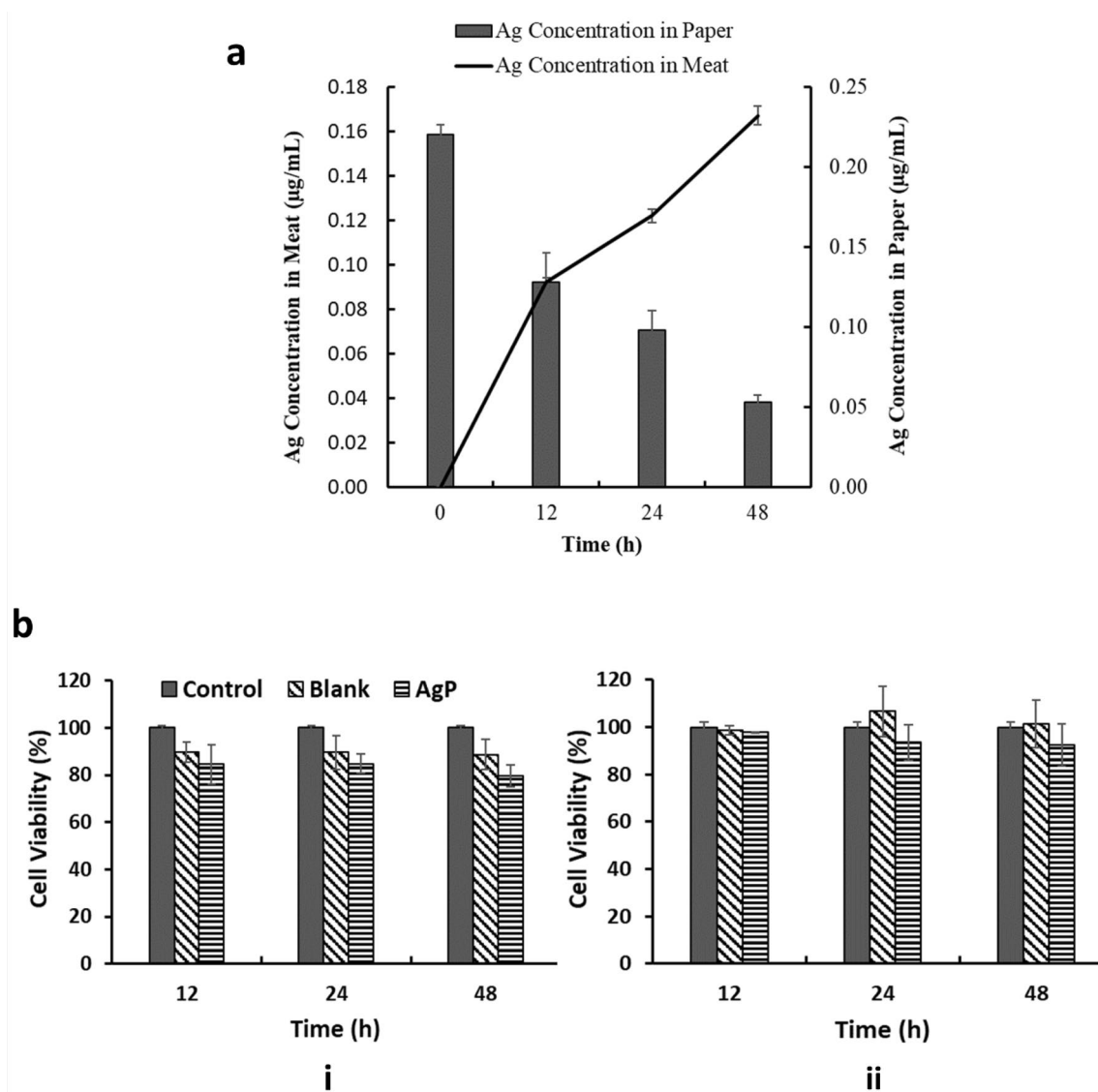


Fig. 5 Release of Ag from the nanocomposite paper and migration into wrapped minced meat at 48 h (a), and in vitro cytotoxicity of release Ag from the nanocomposite and recycled control paper (b)

on human embryonic renal cell HEK293T (i) and human colon cells Caco-2 (ii), showing >80% cell viability after analysis using MTT assay at $p < 0.05$

To further confirm the antimicrobial efficacy of the recycled papers against the test bacterial isolates, a modified method from ISO 20743 was used to mimic the dry state condition experienced with food wraps (Fig. S5). The result confirmed the antimicrobial effects of synthesized nanocomposite paper against Gram-positive *B. cereus* and *L. monocytogenes* and Gram-negative *E. coli* with 2log–3log reduction after 24 h contact with synthesized nanocomposite paper. However, antimicrobial activity of synthesized nanocomposite paper only should an inhibitory effect on *S. aureus*. For all Gram-positive bacteria tested, an increase in CFU/mL was observed, indicating growth of the bacteria on the blank control paper.

Conclusions

The potential recycling of wastepaper and functionalization with silver nanoparticles for the design of active packaging has been demonstrated. The recycled paper demonstrated promising qualities as a suitable source of reusable material for the re-fabrication of paper. Silver nanoparticles incorporated in the paper showed good antimicrobial effects with no cytotoxicity. Thus, the recycled paper could be applied in the packaging of food and other material for the extension of shelf-life and inhibition of microbial mediated spoilage. In addition, recycling and

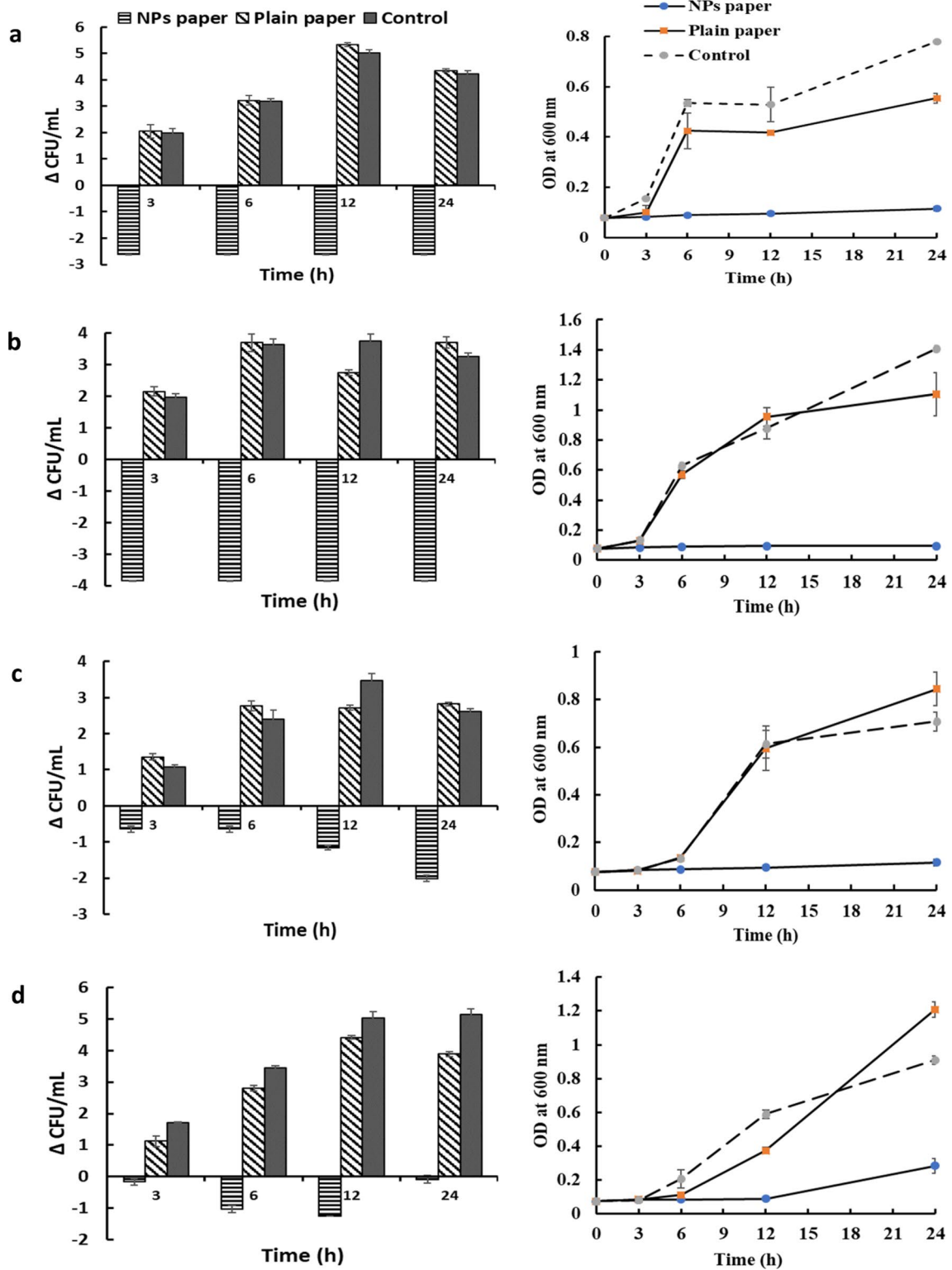


Fig. 6 Bactericidal and growth inhibitory effects of the nanocomposite paper on foodborne pathogenic bacteria. *B. cereus* (a), *E. coli* O157H7 (b), *L. monocytogenes* F2365 (c), and *S. aureus* ATCC 25,923 (d), evaluated using plate count technique and OD measurement

functionalization of wastepaper could be employed as a reusable approach and waste management strategy.

Acknowledgements The study was funded by TRF Senior Research Scholar (Grant No. RTA 6180006) and postdoctoral fellowship, Prince of Songkla University. The authors also wish to thank Dr Nawiya Hui-pao and Dr Nipaporn Konthapakdee of the Department of Physiology, Faculty of Science, Prince of Songkla University for the generous gift of HEK293T and Caco-2 cells.

Compliance with Ethical Standards

Conflict of interest The authors declare that there is no conflict of interest and that all funding bodies have been duly acknowledged.

References

- Battisti, R., Fronza, N., Júnior, A.V., da Silveira, S.M., Damas, M.S., Quadri, M.G.: Gelatin-coated paper with antimicrobial and antioxidant effect for beef packaging. *Food Packag Shelf Life* **11**, 115–124 (2017)
- Kaza, S., Yao, L., Bhada-Tata, P., Van Woerden, F.: *What a Waste 2.0: A Global Snapshot of Solid Waste Management to 2050*. World Bank Publications, Washington (2018)
- Ezeudu, O.B., Agunwamba, J.C., Ezeasor, I.C., Madu, C.N.: Sustainable production and consumption of paper and paper products in Nigeria: a review. *Resources* **8**, 53 (2019)
- Teuber, L., Osburg, V.S., Toporowski, W., Militz, H., Krause, A.: Wood polymer composites and their contribution to cascading utilisation. *J. Clean Prod.* **110**, 9–15 (2016)
- Palombini, F.L., Cidade, M.K., de Jacques, J.J.: How sustainable is organic packaging? A design method for recyclability assessment via a social perspective: a case study of Porto Alegre city (Brazil). *J. Clean Prod.* **142**, 2593–2605 (2017)
- Ren, Q., Zeng, Z., Jiang, Z., Li, H.: Functionalization of renewable bamboo charcoal to improve indoor environment quality in a sustainable way. *J. Clean Prod.* **246**, 119028 (2020)
- Cichello, S.A.: Oxygen absorbers in food preservation: a review. *J. Food Sci. Technol.* **52**, 1889–1895 (2015)
- Bondi, M., Messi, P., Halami, P.M., Papadopoulou, C., de Niederhauser, S.: Emerging microbial concerns in food safety and new control measures. *BioMed Res. Int.* 251512 (2014)
- Nwabor, O.F., Vongkamjan, K., Voravuthikunchai, S.P.: Antioxidant properties and antibacterial effects of *Eucalyptus camaldulensis* ethanolic leaf extract on biofilm formation, motility, hemolysin production, and cell membrane of the foodborne pathogen *Listeria monocytogenes*. *Foodborne Pathog. Dis.* **16**, 581–589 (2019)
- Nasr, A., Saleem Khan, T., Zhu, G.P.: Phenolic compounds and antioxidants from *Eucalyptus camaldulensis* as affected by some extraction conditions, a preparative optimization for GC-MS analysis. *Prep. Biochem. Biotech.* **49**, 464–476 (2019)
- Alghamdi, A.I., Ababutain, I.M.: Phytochemical screening and antibacterial activity of *Eucalyptus camaldulensis*'s leaves and bark extracts. *Asian J. Sci. Res.* **12**, 202–210 (2019)
- CLSI, "M100 performance standards for antimicrobial susceptibility testing," ed: Clinical and Laboratory Standards Institute (2018)
- Jiang, X., Lu, C., Tang, M., Yang, Z., Jia, W., Ma, Y., Wang, H.: Nanotoxicity of silver nanoparticles on HEK293T cells: a combined study using biomechanical and biological techniques. *ACS Omega* **3**, 6770–6778 (2018)
- Lopez de Dicastillo, C., Nerin, C., Alfaro, P., Catala, R., Gavara, R., Hernandez-Munoz, P.: Development of new antioxidant active packaging films based on ethylene vinyl alcohol copolymer (EVOH) and green tea extract. *J. Agric. Food Chem.* **59**, 7832–7840 (2011)
- Paosen, S., Saising, J., Septama, A.W., Voravuthikunchai, S.P.: Green synthesis of silver nanoparticles using plants from Myrtaceae family and characterization of their antibacterial activity. *Mater. Lett.* **209**, 201–206 (2017)
- Loo, Y.Y., Rukayadi, Y., Nor-Khaizura, M.A., Kuan, C.H., Chieng, B.W., Nishibuchi, M., Radu, S.: In vitro antimicrobial activity of green synthesized silver nanoparticles against selected gram-negative foodborne pathogens. *Front. Microbiol.* **9**, 1555 (2018)
- Qasim, M., Udumluck, N., Chang, J., Park, H., Kim, K.: Antimicrobial activity of silver nanoparticles encapsulated in poly-N-isopropylacrylamide-based polymeric nanoparticles. *Int. J. Nanomed.* **13**, 235 (2018)
- Singh, M., Mallick, A., Banerjee, M., Kumar, R.: Loss of outer membrane integrity in Gram-negative bacteria by silver nanoparticles loaded with *Camellia sinensis* leaf phytochemicals: plausible mechanism of bacterial cell disintegration. *Bull. Mater. Sci.* **39**, 1871–1878 (2016)
- Bondarenko, O.M., Sihtmäe, M., Kuzmičiova, J., Ragelienė, L., Kahru, A., Daugelavičius, R.: Plasma membrane is the target of rapid antibacterial action of silver nanoparticles in *Escherichia coli* and *Pseudomonas aeruginosa*. *Int. J. Nanomed.* **13**, 6779 (2018)
- Song, Z., Wu, Y., Wang, H., Han, H.: Synergistic antibacterial effects of curcumin modified silver nanoparticles through ROS-mediated pathways. *Mater. Sci. Eng. C* **99**, 255–263 (2019)
- Liao, S., Zhang, Y., Pan, X., Zhu, F., Jiang, C., Liu, Q., Cheng, Z., Dai, G., Wu, G., Wang, L., Chen, L.: Antibacterial activity and mechanism of silver nanoparticles against multidrug-resistant *Pseudomonas aeruginosa*. *Int. J. Nanomed.* **14**, 1469 (2019)
- Alghoraibia, I., Soukkaiech, C., Zein, R., Alahmad, A., Walter, J.G., Daghestani, M.: Aqueous extract of *Eucalyptus Camaldulensis* leaves as reducing and capping agent in green synthesis of silver nanoparticles. *Curr. Nanomat.* **4**, 1–8 (2019)
- Yu, Z., Wang, W., Kong, F., Lin, M., Mustapha, A.: Cellulose nanofibril/silver nanoparticle composite as an active food packaging system and its toxicity to human colon cells. *Int. J. Biol. Macromol.* **129**, 887–894 (2019)
- Thiagamani, S.M.K., Rajini, N., Siengchin, S., Rajulu, A.V., Hariram, N., Ayrilmis, N.: Influence of silver nanoparticles on the mechanical, thermal and antimicrobial properties of cellulose-based hybrid nanocomposites. *Compos. B Eng.* **165**, 516–525 (2019)
- Qi, H., Cai, J., Zhang, L., Kuga, S.: Properties of films composed of cellulose nanowhiskers and a cellulose matrix regenerated from alkali/urea solution. *Biomacromolecules* **10**, 1597–1602 (2009)
- Kishanji, M., Mamatha, G., Obi Reddy, K., Varada Rajulu, A., Madhukar, K.: In situ generation of silver nanoparticles in cellulose matrix using *Azadirachta indica* leaf extract as a reducing agent. *Int. J. Polym. Anal. Chem.* **22**, 734–740 (2017)
- Sadanand, V., Rajini, N., Satyanarayana, B., Rajulu, A.V.: Preparation and properties of cellulose/silver nanoparticle composites with in situ-generated silver nanoparticles using *Ocimum sanctum* leaf extract. *Int. J. Polym. Anal. Chem.* **21**, 408–416 (2016)
- Swensson, B., Ek, M., Gray, D.G.: Situ preparation of silver nanoparticles in paper by reduction with alkaline glucose solutions. *ACS Omega* **3**, 9449–9452 (2018)
- Dankovich, T.A.: Microwave-assisted incorporation of silver nanoparticles in paper for point-of-use water purification. *Environ. Sci. Nano.* **1**(4), 367–378 (2014)

30. Jafari, N., Karimi, L., Mirjalili, M., Derakhshan, S.J.: Effect of silver particle size on color and antibacterial properties of silk and cotton fabrics. *Fibers Polym.* **17**, 888–895 (2016)
31. Fahmy, H.M., Mosleh, A.M., Elghany, A.A., Shams-Eldin, E., Serea, E.S.A., Ali, S.A., Shalan, A.E.: Coated silver nanoparticles: synthesis, cytotoxicity, and optical properties. *RSC Adv.* **9**, 20118–20136 (2019)
32. Mathew, S., Snigdha, S., Mathew, J., Radhakrishnan, E.: Biodegradable and active nanocomposite pouches reinforced with silver nanoparticles for improved packaging of chicken sausages. *Food Packag. Shelf Life* **19**, 155–166 (2019)
33. Li, H., Cui, R., Peng, L., Cai, S., Li, P., Lan, T.: Preparation of antibacterial cellulose paper using layer-by-layer assembly for cooked beef preservation at ambient temperature. *Polymer* **10**, 15 (2017)
34. Amini, E., Azadfallah, M., Layeghi, M., Talaei-Hassanlou, R.: Silver-nanoparticle-impregnated cellulose nanofiber coating for packaging paper. *Cellulose* **23**, 557–570 (2016)
35. Wu, J., Zheng, Y., Song, W., Luan, J., Wen, X., Wu, Z., Guo, S.: In situ synthesis of silver-nanoparticles/bacterial cellulose composites for slow-released antimicrobial wound dressing. *Carbohydr. Polym.* **102**, 762–771 (2014)
36. Wu, Z., Zhou, W., Pang, C., Deng, W., Xu, C., Wang, X.: Multifunctional chitosan-based coating with liposomes containing laurel essential oils and nanosilver for pork preservation. *Food Chem.* **295**, 16–25 (2019)
37. Vila, L., García-Rodríguez, A., Cortes, C., Marcos, R., Hernandez, A.: Assessing the effects of silver nanoparticles on monolayers of differentiated Caco-2 cells, as a model of intestinal barrier. *Food Chem. Toxicol.* **116**, 1–10 (2018)
38. Böhmert, L., Niemann, B., Thünemann, A.F., Lampen, A.: Cytotoxicity of peptide-coated silver nanoparticles on the human intestinal cell line Caco-2. *Arch. Toxicol.* **86**, 1107–1115 (2012)
39. Tsai, T.T., Huang, T.H., Chang, C.J., Ho, N.Y.J., Tseng, Y.T., Chen, C.F.: Antibacterial cellulose paper made with silver-coated gold nanoparticles. *Sci. Rep.* **7**, 3155 (2017)
40. Praveena, S.M., Karuppiyah, K., Than, L.T.L.: Potential of cellulose paper coated with silver nanoparticles: a benign option for emergency drinking water filter. *Cellulose* **25**, 2647–2658 (2018)

Publisher's Note Springer Nature remains neutral with regard to jurisdictional claims in published maps and institutional affiliations.